Communication

PAMAM Dendrimers Undergo pH Responsive Conformational Changes without Swelling

Yi Liu, Vyacheslav S. Bryantsev, Mamadou S. Diallo, and William A. Goddard III

J. Am. Chem. Soc., **2009**, 131 (8), 2798-2799• DOI: 10.1021/ja8100227 • Publication Date (Web): 06 February 2009

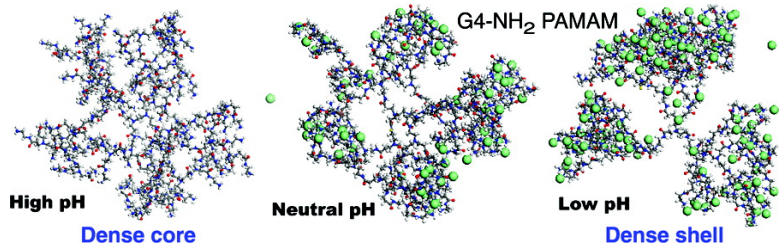

More About This Article

Additional resources and features associated with this article are available within the HTML version:

- Supporting Information
- Access to high resolution figures
- Links to articles and content related to this article
- Copyright permission to reproduce figures and/or text from this article

View the Full Text HTML

J|A|C|S COMMUNICATIONS

Published on Web 02/06/2009

PAMAM Dendrimers Undergo pH Responsive Conformational Changes without Swelling

Yi Liu, Vyacheslav S. Bryantsev, Mamadou S. Diallo, and William A. Goddard III*

Materials and Process Simulation Center (M/C 139-74), California Institute of Technology, 1200 East California Boulevard, Pasadena, California 91125

Received December 23, 2008; E-mail: wag@wag.caltech.edu

Dendrimers[1] provide unique dual characteristics of *ultrasoft colloids* and *structured polymers*,[2,3] making them candidates for a variety of biomedical applications ranging from drug delivery to MRI imaging and gene therapy.[4,5] The pH dependence of size and structure of dendrimers is a critical issue for utilization as drug delivery vehicles in physiological environments (pH = 5 to 7.4). Previous small angle neutron scattering (SANS) experiments on a generation 8 (G8) polyamidoamine (PAMAM)[6] showed a 2% increase of the radius of gyration (R_g) from pH 10.1 to 4.7. This insensitivity of size to the variation of pH was confirmed in the recent SANS experiment on a G4 PAMAM[7] concluding that the R_g is essentially independent of pH (i.e., size change <4%). In contrast, all previous atomistic[8−13] and coarse-grained[14−16] simulations show a significant increase (12−180%) of R_g for PAMAM dendrimers as pH decreases from ∼10 to ∼4.

To resolve this tremendous discrepancy between theory and experiment, we carried out atomistic molecular dynamics (MD) simulations of dendrimers with explicit solvent and counterions using a force field[17] whose intermolecular parameters were optimized using quantum mechanics (QM) [Figures S1−S3 in Supporting Information (SI)]. We calculate that the R_g of the G4-NH_2 PAMAM changes from 21.07 Å at high pH to 22.11 Å at low pH, in excellent agreement with the SANS experiment,[7] 21.41 and 21.49 Å, respectively. Despite the similarity in size, there are dramatic changes in the conformations: The high pH form has a "dense core" (with a maximum density at the dendrimer core and uniform void spacings), whereas ion pairing at low pH leads to a "dense shell" (with maximum density at the dendrimer periphery but nonuniform void spacings).

The G4-NH_2 PAMAM consists of an ethylenediamine ($NH_2CH_2CH_2NH_2$) core, 62 tertiary amine groups, and 124 amide groups in the lower generations and terminated with 64 primary amine groups in the fourth generation. Consistent with the acid−base titration experiments,[18] we model the G4 PAMAM dendrimer at three protonation levels: high pH (>10) with the PAMAM fully deprotonated (uncharged dendrimer), neutral pH (∼7) with all primary amines protonated, and low pH (<5) with all primary and tertiary amines protonated. These dendrimers were solvated with explicit water molecules (∼42 000) and Cl^- counterions in a cubic box (∼110 Å along each dimension). All systems were minimized and then heated to 300 K over 10 ps, followed by MD simulations at 300 K and 1 atm for 1.5 to 2 ns and MD simulations at 300 K with a fixed volume for 1 ns (Figures S4−S5).

For comparison with SANS experiments, R_g is written as

$$\langle R_g^2 \rangle = \frac{1}{W}\left\langle \sum_{i=1}^{N} w_i |r_i - R|^2 \right\rangle$$

where w_i is the weighting factor for atom i, W is a normalization factor, r_i is the position of atom i, and R is the center for the weighting factors. We use as w_i either the neutron scattering length to calculate $R_{g\text{-coh}}$ to compare to SANS experiments or the mass to obtain the mass weighted $R_{g\text{-mass}}$ (see Table 1). Figure 1 shows that the G4 PAMAM dendrimer structures have reached equilibrium with mean values of $R_{g\text{-coh}}$ = 21.07 Å (high pH), 21.43 Å (neutral pH), and 22.11 Å (low pH). Averaging over all three pH values leads to a mean $R_{g\text{-coh}}$ = 21.54 Å and $R_{g\text{-mass}}$ = 21.33 Å for the G4 PAMAM dendrimer in excellent quantitative agreement with the SANS experimental mean $R_{g\text{-coh}}$ = 21.49 Å[7]. The calculated total swelling is 4.9% as pH decreases from high to low, which compares well with the experimental swelling of <4%.

The most complete previous MD simulations[11] for the G4 PAMAM dendrimer found $R_{g\text{-mass}}$ = 16.78 Å (high pH), 17.01 Å (neutral pH), and 19.01 Å (low pH) for a swelling of 12% in distinct disagreement with the SANS experiments. The major difference with our current calculations is that we fitted the intermolecular energy terms in the new force field to QM, finding that the previous Cl^---$^+HN(CH_3)_3$ interaction was ∼17% too weak and 16% too long (see Figures S1 and S2).

More important than the R_g for the applications is the distribution of surface area and chemical characteristics inside the dendrimer and the internal volume. Thus, we calculated the solvent accessible surface area (SASA) and solvent excluded volume (SEV) using various probe radii. Plotting $(SASA)^{1/2}$ and $(SEV)^{1/3}$ as functions of probe radius (Figures S6−S10) shows that, for a probe radius of p > 7 Å, $(SASA)^{1/2}$ and $(SEV)^{1/3}$ are proportional to probe radius, indicating that only the exterior surface of the dendrimer is sampled and suggesting that molecules with a radius > 7 Å would not fit inside the dendrimer. The deviation in SASA and SEV at smaller probe radii (Figures S6 and S7) measures the internal cavities within the dendrimer. At p = 1.4 Å (H_2O), the SASA analysis indicates an internal surface area (A_{int}) of 3778.6 $Å^2$ or 1600.9 m^2/g and a void volume (V_{int}) of 36776.9 $Å^3$ or 1.56 × 10^{-6} m^3/g at neutral pH (Table 1). The A_{int} decreases by 63.5% from high to low pH, while the V_{int} decreases by 21.0% despite an increase of $R_{g\text{-coh}}$ by

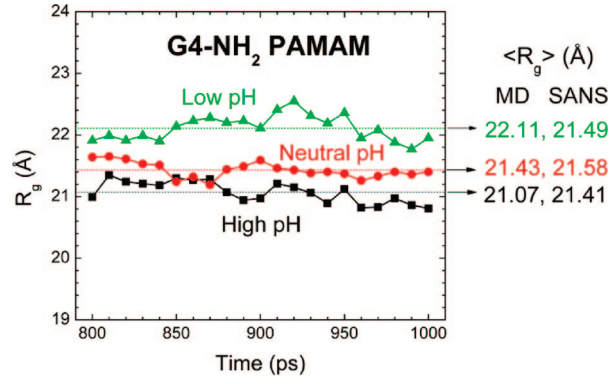

Figure 1. Radius of gyration ($R_{g\text{-coh}}$) of G4-NH_2 PAMAM for the last 200 ps of MD. Dashed lines show the average $\langle R_g \rangle$ over the 200 ps, compared with the SANS values.[7]

10.1021/ja8100227 CCC: $40.75

Table 1. Radius of Gyration (R_g), Solvent Accessible Surface Area (SASA), and Solvent Excluded Volume (SEV) of G4-NH_2 PAMAM at High, Neutral, and Low pH

PAMAM	SANS (Å)[7]	$R_{g\text{-coh}}$	$R_{g\text{-mass}}$	$R_{gN\text{-mass}}$	R_{SASA} (Å)	R_{SEV} (Å)	SASA (Å^2)[a]	SEV (Å^3)[a]	A_{int} (Å^2)[a]	V_{int} (Å^3)[a]
high pH	21.41 ± 0.74	21.07 ± 0.17	20.90 ± 0.17	24.66 ± 0.26	28.95	26.01	17239.2	44520.8	5696.1	41421.1
neutral pH	21.58 ± 0.41 (0.8%)[b]	21.43 ± 0.13 (1.7%)	21.25 ± 0.12 (1.7%)	23.84 ± 0.20 (−3.3%)	28.34 (−2.1%)	25.19 (−3.2%)	14862.4 (−13.8%)	41680.3 (−6.4%)	3778.6 (−33.7%)	36776.9 (−11.2%)
low pH	21.49 ± 0.25 (0.4%)[b]	22.11 ± 0.20 (4.9%)	21.83 ± 0.20 (4.4%)	26.14 ± 0.29 (6.0%)	27.89 (−3.7%)	24.57 (−5.5%)	12830.7 (−25.6%)	40376.2 (−9.3%)	2079.8 (−63.5%)	32719.8 (−21.0%)

[a] A probe radius of 1.4 Å was used as the vdW radius of a water molecule to calculate the SASA and SEV. [b] Percentage change using high pH data as baseline.

4.9%. This further illustrates the dramatic change in internal configurations with pH. The variations in SASA can be used to derive an effective outer radius, e.g., R_{SASA} = 28.34 Å at neutral pH (see Table 1 and Figure S6), which can be considered the effective macromolecule size that would be found in size exclusion chromatography (SEC). The ratio $R_{SASA}/R_{g\text{-mass}}$ = 1.33 can be compared to R_{outer}/R_g = 1.29 for a uniform sphere. Considering just the primary amine N atoms leads to R_{gN} = 23.84 Å (neutral pH), which is 84.1% of the R_{SASA}, suggesting backfolding of the terminal groups.

The radial density distribution profile (Figure 2) shows that the maximum density of the dendrimer shifts from 10 Å at high pH to 18 Å at neutral or low pH. This mass migration to the periphery of the dendrimers is driven by strong intramolecular hydrogen bonding within the dendrimer−water−counterion systems, which leads to dense packing in the outer shell at low pH as shown in Figure 2. One might expect this pH-induced outward mass redistribution within the dendrimer to increase its moment of inertia and R_g. However, the shrinking of the outer diameter of the dendrimer at low pH, indicated by the decreasing R_{SASA}, would tend to decrease R_g. Thus, the independence of the R_g upon variation of pH arises from a competition between geometrical shrinking and outward mass redistribution. This pH-induced conformational change from a "dense core" (high pH) to a "dense shell" (low pH) suggests how PAMAM dendrimers might be used as drug delivery vehicles where encapsulation and release of guest molecules (e.g., drugs) can be controlled using pH as the trigger.

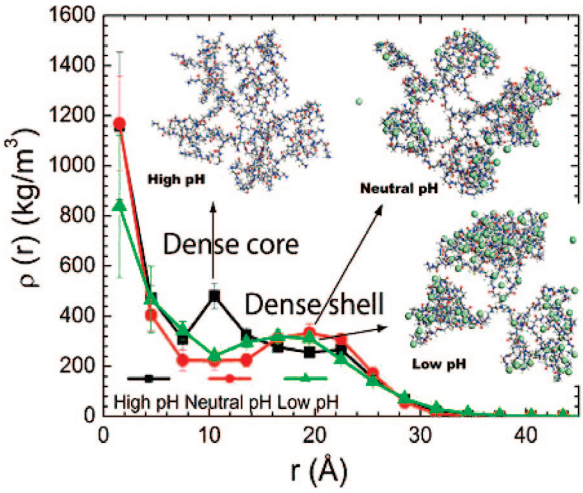

Figure 2. Radial density distribution of G4-NH_2 PAMAM dendrimer at various pH values (using the center of mass of the dendrimer as the reference and averaged over 200 ps). Snapshots from MD simulations are shown in the insert.

Acknowledgment. We are grateful to Dr. Wei-Ren Chen for initiating this collaboration between Oak Ridge National Laboratory (LDRD 05125) and Caltech and for many fruitful discussions.

Supporting Information Available: The solvent accessible area and solvent excluded volume of PAMAM as functions of probe radius, the relevant force field parameters, and the thermodynamic properties in MD simulations. This material is available free of charge via the Internet at http://pubs.acs.org.

References

(1) (a) Tomalia, D. A.; Naylor, A. M.; Goddard, W. A. *Angew. Chem., Int. Ed. Engl.* **1990**, *29*, 138–175. (b) Naylor, A. M., Goddard, W. A., III. In *Biocatalysis and Biomimetics*; Burrington, J. D., Clark, D. S., Eds.; ACS Symposium Series 392; American Chemical Society: Washington, DC, 1989; Chapter 6, pp 65−87. (c) Naylor, A. M.; Goddard, W. A., III; Kiefer, G. E.; Tomalia, D. A. *J. Am. Chem. Soc.* **1989**, *111*, 2339.
(2) Likos, C. N. *Soft Matter* **2006**, *2*, 478–498.
(3) Ballauff, M.; Likos, C. N. *Angew. Chem., Int. Ed.* **2004**, *43*, 2998–3020.
(4) Majoros, I. J.; Williams, C. R.; Baker, J. R. *Curr. Top. Med. Chem.* **2008**, *8*, 1165–1179.
(5) Smith, D. K. *Curr. Top. Med. Chem.* **2008**, *8*, 1187–1203.
(6) Nisato, G.; Ivkov, R.; Amis, E. J. *Macromolecules* **2000**, *33*, 4172–4176.
(7) Chen, W. R.; Porcar, L.; Liu, Y.; Butler, P. D.; Magid, L. J. *Macromolecules* **2007**, *40*, 5887–5898.
(8) Opitz, A. W.; Wagner, N. J. *J. Polym. Sci., Part B: Polym. Phys.* **2006**, *44*, 3062–3077.
(9) Lee, I.; Athey, B. D.; Wetzel, A. W.; Meixner, W.; Baker, J. R. *Macromolecules* **2002**, *35*, 4510–4520.
(10) Maiti, P. K.; Goddard, W. A. *J. Phys. Chem. B* **2006**, *110*, 25628–25632.
(11) Maiti, P. K.; Cagin, T.; Lin, S. T.; Goddard, W. A. *Macromolecules* **2005**, *38*, 979–991.
(12) Lin, S. T.; Maiti, P. K.; Goddard, W. A. *J. Phys. Chem. B* **2005**, *109*, 8663–8672.
(13) Maiti, P. K.; Cagin, T.; Wang, G. F.; Goddard, W. A. *Macromolecules* **2004**, *37*, 6236–6254.
(14) Welch, P.; Muthukumar, M. *Macromolecules* **1998**, *31*, 5892–5897.
(15) Giupponi, G.; Buzza, D. M. A.; Adolf, D. B. *Macromolecules* **2007**, *40*, 5959–5965.
(16) Blaak, R.; Lehmann, S.; Likos, C. N. *Macromolecules* **2008**, *41*, 4452–4458.
(17) Mayo, S. L.; Olafson, B. D.; Goddard, W. A. *J. Phys. Chem.* **1990**, *94*, 8897–8909.
(18) Cakara, D.; Kleimann, J.; Borkovec, M. *Macromolecules* **2003**, *36*, 4201–4207.

JA8100227